J. Cent. South Univ. (2021) 28: 669−678
DOI: https://doi.org/10.1007/s11771-021-4636-7

Springer

Highly-dispersed iron element decorated nickel foam synthesized by an acid-free and one-pot method for enzyme-free glucose sensor

ZHANG Yin-he(张银河)[1], HUANG Su-ping(黄苏萍)[1], XIAO Qi(肖奇)[2]

1. State Key Lab of Powder Metallurgy, Central South University, Changsha 410083, China;
2. School of Minerals Processing and Bioengineering, Central South University, Changsha 410083, China

Abstract: The highly-dispersed iron element decorated Ni foam was prepared by simple immersion in a ferric nitrate solution at room temperature without using acid etching, and characterized by X-ray powder diffraction (XRD), scanning electron microscopy (SEM), EDAX spectrum (EDAX mapping) and Raman spectroscopy. The EDAX spectrum illustrated that iron element was highly-dispersed over the entire surface of nickel foam, and the Raman spectroscopy revealed that both Ni—O and Fe—O bonds were formed on the surface of the as-prepared electrode. Moreover, the iron element decorated Ni foam electrode can be used as non-enzymatic glucose sensor and it exhibits not only an ultra-wide linear concentration range of 1−18 mmol/L with an outstanding sensitivity of 1.0388 mA·mmol/(L·cm^2), but also an excellent ability of stability and selectivity. Therefore, this work presents a simple yet effective approach to successfully modify Ni foam as non-enzymatic glucose sensor.

Key words: one-pot synthesis; acid-free; highly-dispersed iron element; nickel foam; non-enzymatic glucose sensor

Cite this article as: ZHANG Yin-he, HUANG Su-ping, XIAO Qi. Highly-dispersed iron element decorated nickel foam synthesized by an acid-free and one-pot method for enzyme-free glucose sensor [J]. Journal of Central South University, 2021, 28(3): 669−678. DOI: https://doi.org/10.1007/s11771-021-4636-7.

1 Introduction

Diabetes is one of the most common and deadliest diseases, with which several millions of people worldwide were living. It is very important to precisely monitor blood glucose level in order to manage diabetes effectively. Among the various methods applied for the quantitative detection of glucose, non-enzymatic electrochemical glucose sensors (NEGSs) have received increasing attention due to their significant advantages such as high stability, specificity and non-toxicity [1−3]. At present, various micro/nanomaterials, including noble metals, transition metal oxides or hydroxides, transition metal chalcogenides, transition metal phosphate, etc, have been intensively studied toward NEGSs [4−8]. Nevertheless, it is a great challenge to fabricate NEGSs with wide linear range, high sensitivity, stability and specificity. For example, noble metals exhibit wide linear range [9], but they have drawbacks such as the chloride ion poisoning, low selectivity, and high cost. All of the transition metal oxides or hydroxides, chalcogenides, phosphate-based sensors are proved unaffected by chloride ion concentration. However, some sensors (e.g., Co_3O_4 nanowires [10], nickel-doped FeS_2 [11]) exhibited wide linear range but low sensitivity, while the others (e.g., $Ni(OH)_2$ nanowires [12], NH_4NiPO_4 [13, 14]) showed high sensitivity but narrow linear range. Therefore, it is crucial to develop novel micro/nanomaterials based

Foundation item: Project(2019zzts684) supported by the Fundamental Research Funds for the Central Universities, China
Received date: 2020-09-15; **Accepted date:** 2021-01-08
Corresponding author: XIAO Qi, PhD, Associate Professor; Tel: +86-731-88830543; E-mail: xiaoqi88@csu.edu.cn; ORCID: https://orcid.org/0000-0003- 4679-8276

NEGSs with wide linear range, high sensitivity, high specificity and high stability.

It is well known that the self-supported electrodes on various conductive substrates (such as graphene [15], Cu [16], Fe [17], Co [18], glassy carbon [19] and Ni [20]) can effectively improve the sensitivity of NEGSs. Among these self-supported electrodes, Ni-based electrodes exhibit excellent electrocatalytic activity resulting from the redox couple of $Ni(OH)_2$/NiOOH in alkaline medium [14, 21]. Up to now, various methods have been reported to fabricate self-supported Ni-based electrodes, including hydrothermal method [22], electrochemical deposition [23], and high-temperature calcination [24]. Nevertheless, the above-mentioned synthesis methods require harsh synthesis conditions (e.g., high temperature, additional electricity input). Therefore, the development of a simple method for one-pot construction of a high-performance NEGSs remains a significant challenge.

Herein, we fabricate a high-performance self-supported Ni foam-based NEGSs by simple immersion in a ferric nitrate ($Fe(NO_3)_3$) solution at room temperature. Specifically, the iron element is highly dispersed on the Ni foam (NF) surface. Moreover, the as-prepared iron decorated NF electrodes exhibit the excellent electrochemical performance and demonstrate the potential for facilitating the development of non-enzymatic glucose sensors with wide linear range, high sensitivity and excellent selectivity and stability.

2 Experimental section

2.1 Preparation of iron element decorated nickel foam

The highly dispersed iron decorated electrode was fabricated by a facile and acid-free process. Typically, a piece of nickel foam (1 cm×1 cm) was cleaned with alcohol and deionized water. Then, the cleaned nickel foam (NF) was fully immersed in 20 mL freshly prepared solution containing different concentrations (10, 20, 30 mmol/L) of $Fe(NO_3)_3$ at room temperature (25 °C) for different time (4, 8, 12 h), respectively. Finally, the iron element decorated NF samples were rinsed with deionized water and dried at 50 °C. The obtained samples were named as Fe/NF-*X*-*Y* (*X* means the concentrations of $Fe(NO_3)_3$ solutions and *Y* means immersion time). In addition, Ni foam (NF) was further cleaned with 2 mol/L HCl solution for 10 min, and the obtained acid-treated NF (ANF) was immersed in 20 mmol/L $Fe(NO_3)_3$ solutions for 8 h, and the obtained sample was named as Fe/ANF-20-8.

2.2 Material characterization

The XRD patterns of the samples were recorded with a DX-2700 X-ray powder diffractometer (XRD) with Cu Kα radiation (λ= 1.54056 Å). The morphology, structure and energy dispersive X-ray analysis (EDAX) of these electrodes were characterized by field emission scanning electron microscopy (SEM, Nova Nano SEM230). The Raman spectra were obtained by HR800 laser Raman spectroscopy (Jobin Yvon, France) to determine the Ni—O and Fe—O bonds. The excitation source was He-Ne ion laser with excitation wavelength of 632.8 nm and the laser power on the sample was 10 mW.

2.3 Electrochemical measurement

The electrochemical performances of the electrodes were measured at room temperature on an electrochemical work station (Gamry Reference 600). The cyclic voltammetry (CV) was measured in 150 mL of 0.3 mol/L NaOH solution at a sweep rate of 50 mV/s in the potential range from −0.2 to 0.9 V. The as-synthesized electrode (1 cm×1 cm) was used as the working electrode, a Pt foil electrode as the counter electrode and Ag/AgCl electrode as the reference electrode in the standard three electrode system.

3 Results and discussion

3.1 Materials characterization

As schematically illustrated in Figure 1, at first a piece of nickel foam was cleaned only with alcohol and deionized water without acid etching. Then, the nickel foam was immersed in $Fe(NO_3)_3$ solutions at room temperature for several hours. Finally, the as-prepared electrodes were cleaned with deionized water and dried at 50 °C. The characterization results of Fe/NF-20-8 are shown in Figure 2. Notably, according to the Raman spectra (Figure 2(f)), both Ni—O and Fe—O bonds were formed on the surface of NF during the immersion in the $Fe(NO_3)_3$ solutions. Thus, highly dispersed

iron element decorated nickel foam electrode was obtained.

Typically, NF was immersed in a 20 mmol/L aqueous $Fe(NO_3)_3$ solution for 8 h, and the obtained sample was named as Fe/NF-20-8. The SEM image in Figure 2(a) shows that the surface of Fe/NF-20-8 is as smooth as NF (Figure 3(a)). The XRD patterns of NF and Fe/NF-20-8 electrodes are shown in Figure 3(b). The diffraction peaks of NF and Fe/NF-20-8 are all corresponding to the pure metal Ni (JCPDS No. 04-0850) and no other impurity peaks are observed. The results of SEM and XRD indicate that there are no visible substances on the surface and the content of iron is extremely low.

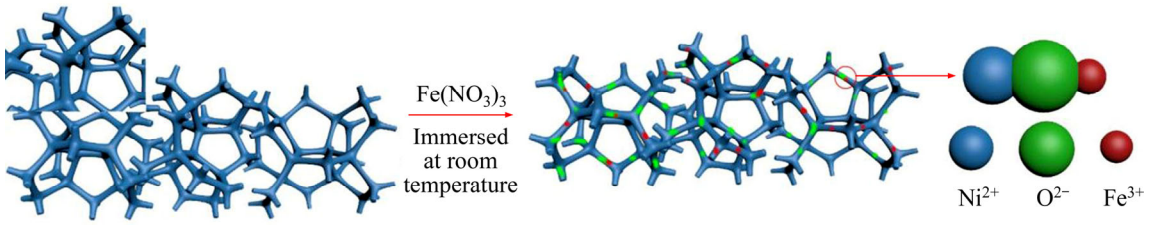

Figure 1 Schematic illustration for fabrication of iron element decorated Ni-based electrode

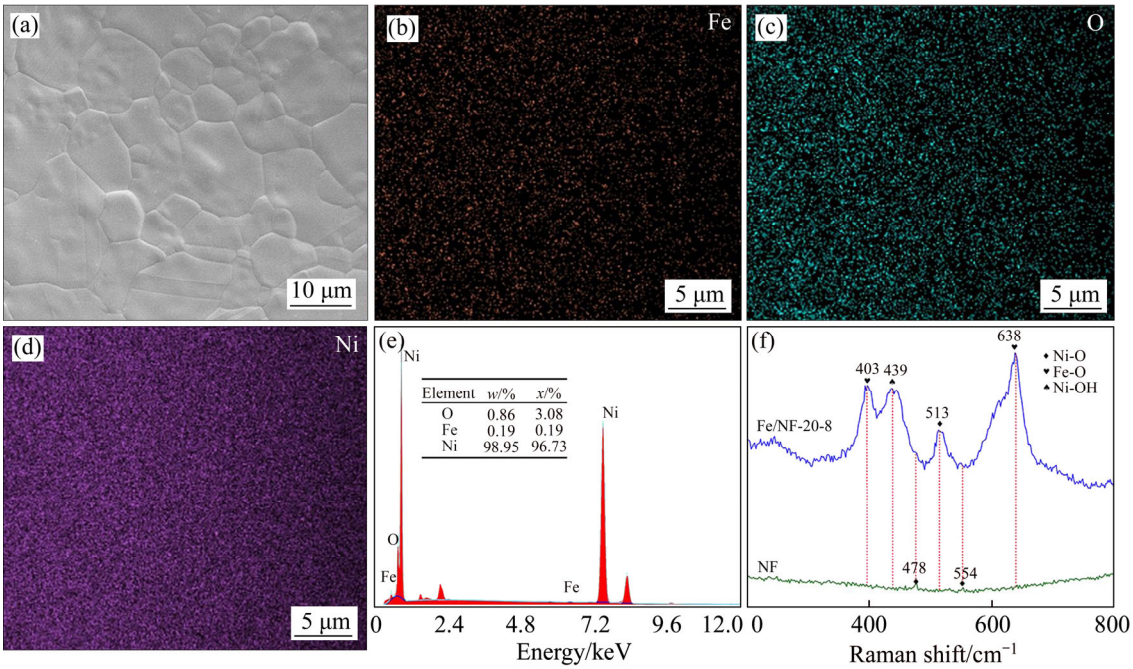

Figure 2 (a) SEM image of Fe/NF-20-8; EDAX mapping images of Fe element (b), O element (c), Ni element (d); (e) EDAX mapping spectrum of Fe/NF-20-8; (f) Raman spectra of NF and Fe/NF-20-8

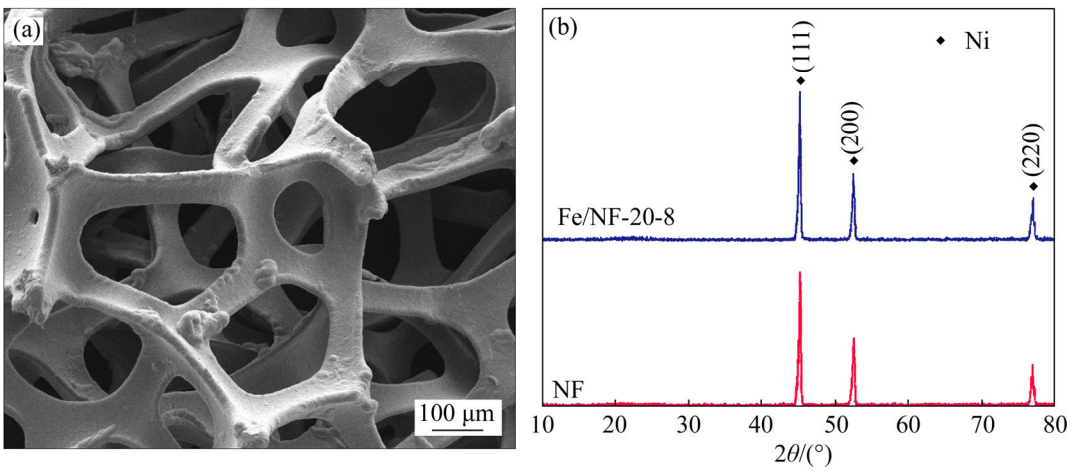

Figure 3 (a) SEM image of Ni foam; (b) XRD pattern of NF and Fe/NF-20-8 electrodes

And the elements mapping images have shown the uniform distribution of Fe, O and Ni on the surface of Fe/NF-20-8 (as shown in Figures 2(b)−(d)). Moreover, the EDAX pattern of Fe/NF-20-8 (Figure 2(e)) provides the typical signal of Fe, O and Ni elements, and the atomic percents of iron, oxygen and nickel are 0.19%, 3.08% and 96.73%, respectively. Therefore, the above results confirm the presence of Fe on the surface of NF.

The typical Raman spectra of NF and Fe/NF-20-8 are presented in Figure 2(f). Two weak Raman scattering peaks at around 478 and 554 cm^{-1} are observed for the pristine NF, which can be assigned to the bending and stretching vibration mode of N—O in Ni(OOH) [25]. In contrast, the Fe/NF-20-8 sample exhibits four sharp peaks at 403, 439, 513 and 638 cm^{-1}. The peaks at 439 and 513 cm^{-1} can be attributed to the symmetric Ni—OH stretching mode and the vibration of Ni—O stretching mode, respectively [26]. In addition, the peaks at 403 and 638 cm^{-1} are assigned to Fe—O vibrations [27]. These results have revealed both Ni—O and Fe—O bonds formed on the surface of the Fe/NF-20-8 sample.

3.2 Electrochemical performance of as-prepared electrodes

In this work, the electrocatalytic performance of the as-prepared electrode was assessed by CV measurements in 0.3 mol/L NaOH solution at a scan rate of 50 mV/s. The CV curve of Fe/NF-20-8 is shown in Figure 4(a). The observed stable oxidation peak currents of as-synthesized electrodes changed dramatically and increased regularly. It exhibits a positive shift with increasing concentrations of glucose solution, and the corresponding calibration curves of the response current density against glucose concentration are shown in Figure 4(b), indicating that Fe/NF-20-8 presented a linear dependence on glucose concentration in a range between 1 and 18 mmol/L. The linear equation is presented as $J=1.0388\times10^{-6}\ C_{glucose}+1.546\times10^{-2}$ ($R^2=0.992$) with a sensitivity of 1.0388 mA·mmol/(L·cm^2). Therefore, a small

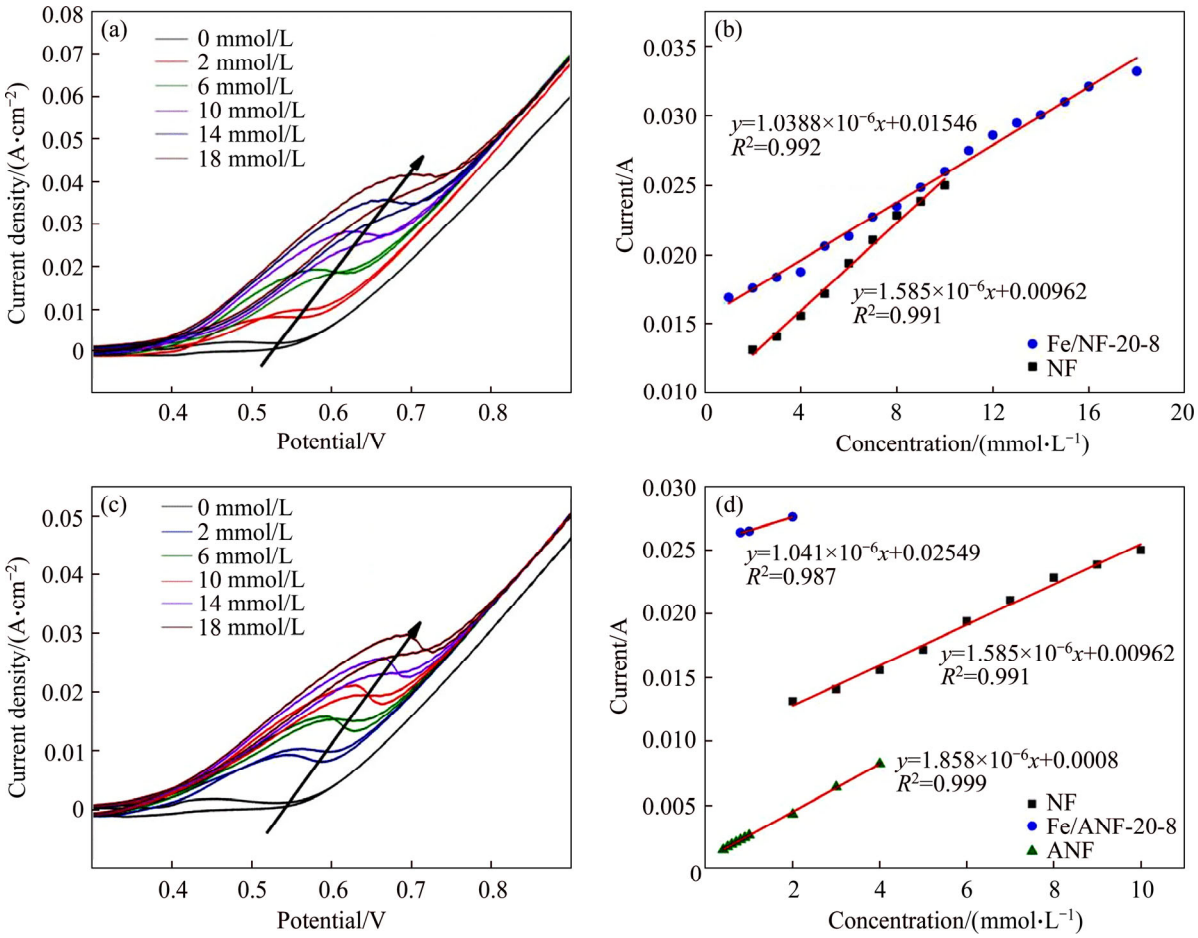

Figure 4 (a) CV curve of Fe/NF-20-8; (b) Calibration curves of Fe/NF-20-8 and nickel foam; (c) CV curves of Ni foam electrode; (d) Calibration curves of ANF, Fe/ANF-20-8 and NF

amount of Fe can improve the electrochemical performance. Above all, the iron element decorated Ni foam electrode can be used as non-enzymatic glucose sensor and it exhibits an ultra-wide linear concentration range of 1−18 mmol/L. However, the detailed mechanism about the role of iron element should be further investigated in the future.

In addition, the CV curve of Ni foam is shown in Figure 4(c), and the corresponding current response of Ni foam electrode is linear with glucose concentration over a range of 2−10 mmol/L. Its linear equation is presented as J=1.585×10^{-6} $C_{glucose}$+9.62×10^{-3} (R^2=0.991) with a sensitivity of 1.585 mA·mmol/(L·cm^2). It is obvious that Fe/NF-20-8 has a wider linear range than NF. In addition, we investigated the effect of acid cleaning pre-treatment of Ni foam on the electrocatalytic performance (Figure 4(d)). Fe/ANF-20-8 exhibits a narrow linear range (covered from 0.8 to 2 mmol/L) and its linear equation is presented as J=1.041×10^{-6} $C_{glucose}$+2.549×10^{-2} (R^2=0.987) with a sensitivity of 1041 μA·mmol/(L·cm^2). Moreover, ANF exhibits a narrow linear range of 0.4−4 mmol/L with sensitivity of 1.858 mA·mmol/(L·cm^2). Its linear equation is presented as J=1.858×10^{-6} $C_{glucose}$+ 0.8×10^{-3} (R^2=0.999). It is found that either ANF or Fe/ANF-20-8 electrode exhibited much narrower linear range than NF, indicating that the general acid cleaning pre-treatment of Ni foam led to the inferior electrocatalytic performance in this case.

The CV curves of Fe/NF-20-4 and Fe/NF-20-12 are shown in Figures 5(a) and (b), respectively. And the corresponding current response of Fe/NF-20-4 is linear with glucose concentration over a range of 1−6 mmol/L (R^2= 0.981) with a sensitivity of 1.675 mA·mmol/(L·cm^2) and Fe/NF-20-12 is 1−7 mmol/L (R^2=0.993) with a sensitivity of 1.3596 mA·mmol/(L·cm^2) (Figure 5(c)). Among them, Fe/NF-20-8 shows the best electrocatalytic properties. Thus, the immersion time of 8 h can be a suitable condition for our electrodes.

The electrochemical results of electrodes which were immersed in different concentrations of $Fe(NO_3)_3$ solutions for 8 h are shown in Figures 5(d)−(f). The anodic peak currents of Fe/NF-10-8 (Figure 5(d)) and Fe/NF-30-8 (Figure 5(e)) electrodes changed dramatically and increased regularly with the addition of glucose concentration. And Fe/NF-10-8 exhibits linear range (covered from 2−12 mmol/L, R^2=0.995) with a sensitivity of 1.484 mA·mmol/(L·cm^2), and Fe/NF-30-8 exhibits linear range (covered from 1−6 mmol/L, R^2=0.997) with a sensitivity of 1.735 mA·mmol/(L·cm^2) (Figure 5(f)). It is obvious that the Fe/NF-20-8 electrode shows better electrochemical performances compared with Fe/NF-10-8 and Fe/NF-30-8 electrodes. Thus, the optimized concentration of $Fe(NO_3)_3$ solutions should be 20 mmol/L. And the electrocatalytic performance of as-prepared electrodes is compared with other reported nickel-based glucose sensors [28−30] (shown in Table 1). It is found that our electrodes show a wider linear range and a high sensitivity to glucose detection.

The kinetic analysis of the as-prepared electrodes for non-enzymatic glucose detection was investigated by CV and chronoamperometry response in 0.3 mol/L NaOH solution, as shown in Figure 6. The CVs of the Fe/NF-20-8 at various scan rates in the presence of 5 and 15 mmol/L glucose are illustrated in Figures 6(a) and (c), respectively. With the increase of scan rates, the cathodic peak appeared gradually. It is indicated that the oxidation of glucose may belong to a slow process [31]. As shown in Figures 6(b) and (d), the anodic peak currents of as-prepared electrodes in the presence of 5 mmol/L glucose and and 15 mmol/L glucose are linearly proportional to the square root of scan rate, suggesting a typical diffusion-controlled reaction. In addition, Fe/NF-20-8 shows better linear relationship, indicating the diffusion-controlled process kinetically favored Fe/NF-20-8.

Meanwhile, the plots of peak currents versus scan rates with 5 mmol/L glucose and 15 mmol/L glucose are shown in Figures 7(a) and (b), respectively. It is found that the Fe/NF-20-8 sample shows the worse correlation coefficients, suggesting that the peak currents are not linearly proportional to the scan rates. In addition, Figures 7(c) and (d) show the plots of anodic peak potential versus the natural logarithm of the scan rates. It is obvious that the correlation coefficients are worse and the peak potentials are not linearly proportional to the scan rates. In a word, the above-mentioned results of both Figures 6 and 7 imply that the glucose

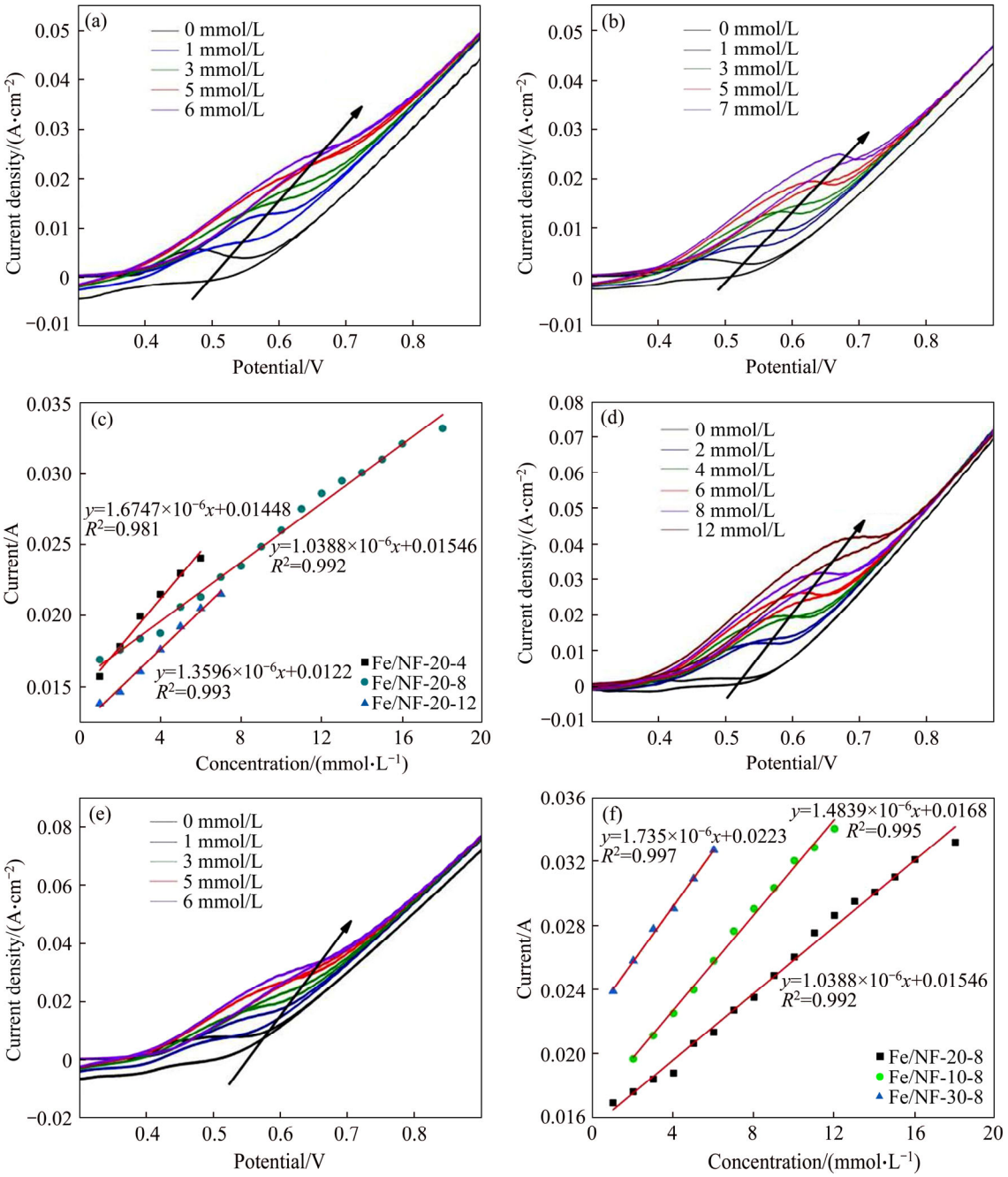

Figure 5 CV curves of Fe/NF-20-4 (a), Fe/NF-20-12 (b), Fe/NF-10-8 (d), and Fe/NF-30-8 (e); Corresponding calibration curves of Fe/NF-20-4, Fe/NF-20-8 and Fe/NF-20-12 (c) and Fe/NF-10-8, Fe/NF-20-8 and Fe/NF-30-8 (f)

Table 1 Comparison of our electrodes with other reported nickel-based glucose sensors

Sample	Linear range/(mmol·L^{-1})	Sensitivity/(μA·mmol·L^{-1}·cm^{-2})	Ref.
$Ni(OH)_2$ nanowires	0.1−6	1598	[12]
3D-flowerlike NH_4NiPO_4	1×10^{-3}−1, 2−5	6135, 2205	[13]
H_2O_2/NH_4NiPO_4	1×10^{-3}−1, 2−4	1136.1, 3579.9	[14]
Ni_3Se_2/NS/Ni foam	0.2510^{-3}−6.335	5962	[22]
GLAD NiO	0.5×10^{-3}−9	4400	[28]
NiO HPA	0.0025−1.1	1323	[29]
NiO/NS@NR/Ni foam	0.751×10^{-3}−3.837	2739.5	[30]
Fe/NF-20-8	1−18	1038.8	This study

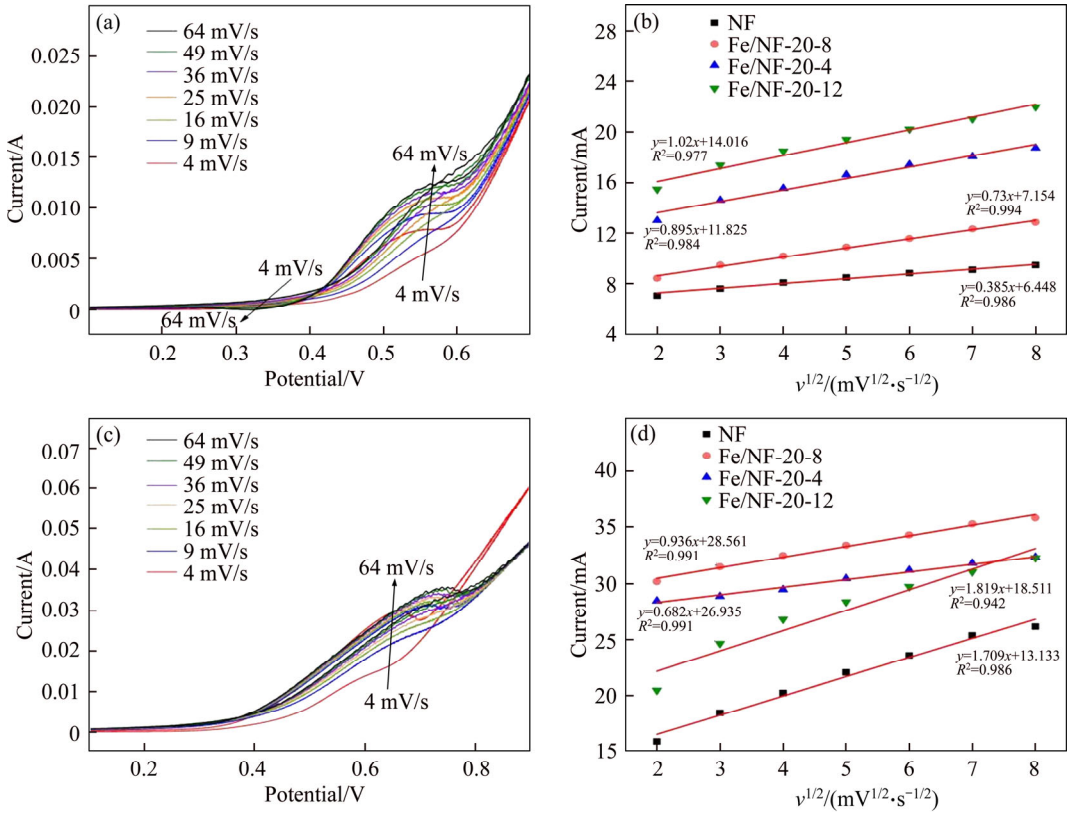

Figure 6 CV curves of Fe/NF-20-8 with 5 mmol/L glucose (a) and 15 mmol/L glucose (c) at various scan rates; Corresponding plots of anodic peak currents versus square root of potential scan rate in the presence of 5 mmol/L (b) and 15 mmol/L glucose (d)

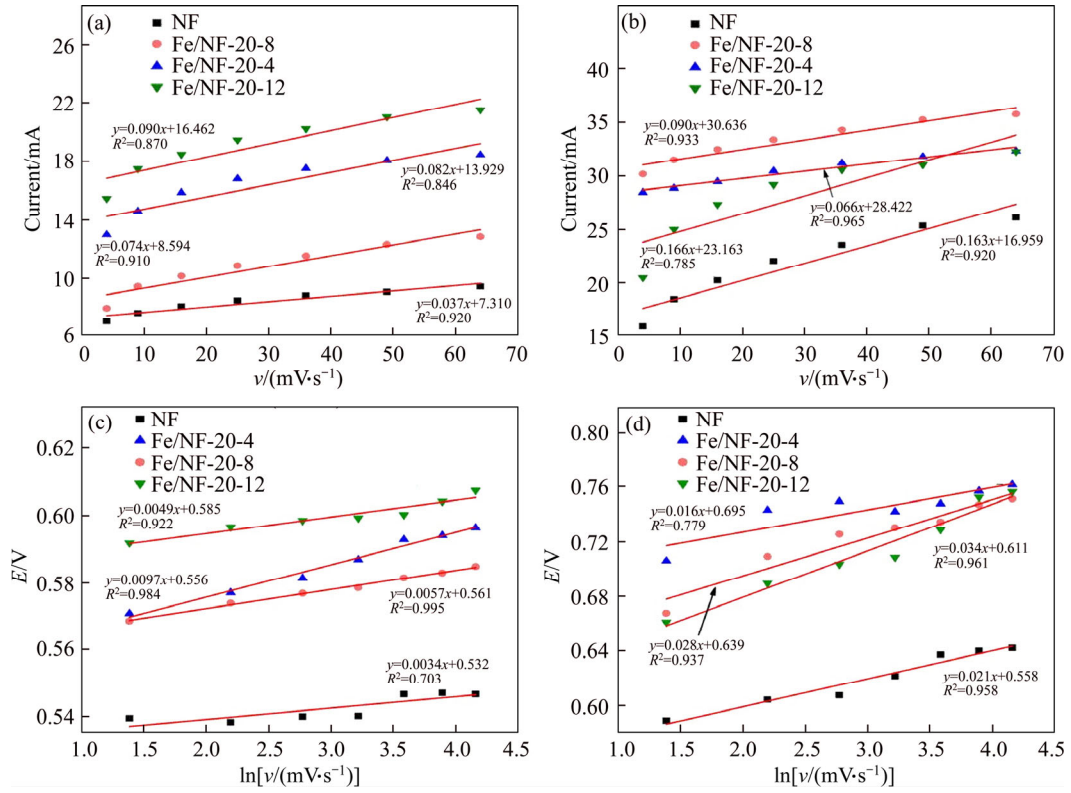

Figure 7 Plots of peak currents of as-prepared electrodes versus scan rates in the presence of 5 mmol/L (a) and 15 mmol/L glucose (b); Plot of peak potential versus logarithm of scan rates for anodic peaks in the presence of 5 mmol/L (c) and 15 mmol/L glucose (d)

oxidation over Fe/NF-20-8 is diffusion-controlled rather than surface-controlled [32].

In addition, the plots of lg$J$ versus lg$v$ are shown in Figures 8(a) and (b) in the presence of 5 and 15 mmol/L glucose, respectively. According to the previous literature [33], if a slope of 0.5 is found, the reaction is purely diffusion-controlled. In our case, the slope results (shown in Figure 8) are less than the predicted value (0.5) of a purly diffusion- controlled process, which infers kinetics limitation in the overall reaction [33].

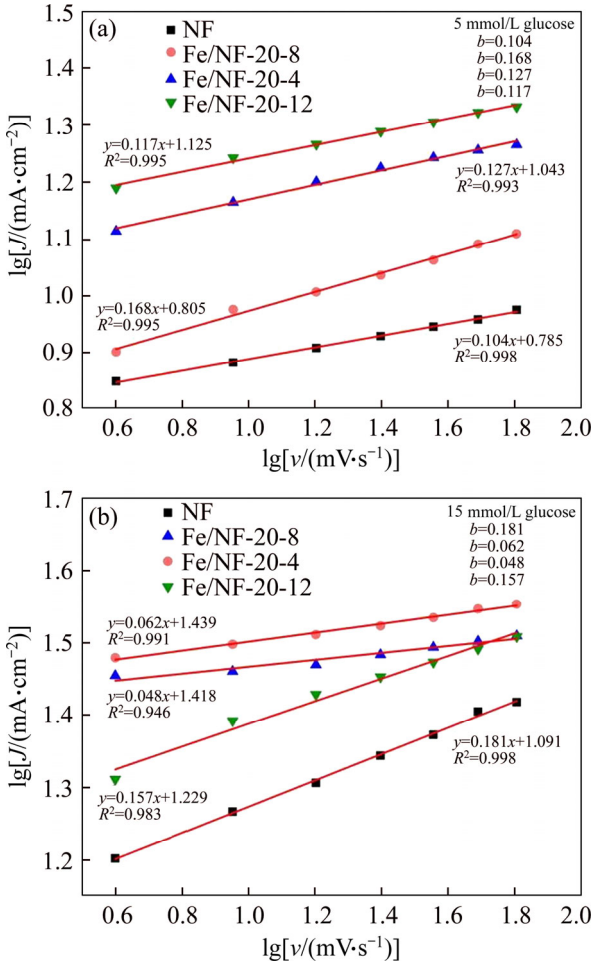

Figure 8 Plots of lg$J$ versus lg$v$ of as-prepared electrodes with 5 mmol/L glucose (a) and 15 mmol/L glucose (b)

To evaluate the performance of anti-interference, five interfering substances, including lactose, KCl, NaCl, urea and UA were measured to glucose. As shown in Figure 9, after adding 0.1 mmol/L lactose and 0.1 mmol/L urea, the responding current is elevated slightly while the current is reduced a little for adding 0.1 mmol/L other compounds. Therefore, it is indicated that the Fe/NF-20-8 electrode exhibited good selectivity.

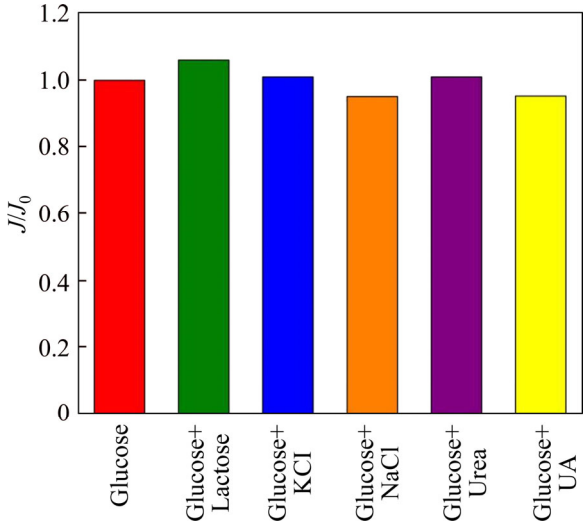

Figure 9 Histogram of anti-interference performance of Fe/NF-20-8 in 0.3 mol/L NaOH solution containing 4 mmol/L glucose, 0.1 mmol/L lactose, 0.1 mmol/L KCl, 0.1 mmol/L NaCl, 0.1 mmol/L urea and 0.1 mmol/L UA (J_0 and J are the current densities of Fe/NF-20-8 before and after the addition of compounds)

4 Conclusions

In summary, an acid-free and facile one-pot method was successfully developed to construct Ni-based non-enzymatic glucose sensor. The iron was highly dispersed on the surface of Ni foam after ferric nitrate solution treatment. As a consequence, the Fe/NF-20-8 electrode exhibits excellent electrochemical performance with a wide linear range (1−18 mmol/L) and high sensitivity (1.0388 mA·mmol/(L·cm^2)), and some kinetic for the oxidation of glucose was obtained, suggesting a typical diffusion-controlled reaction. Furthermore, Fe/NF-20-8 electrode exhibits an outstanding stability and selectivity. Thus, the highly dispersed iron decorated Ni foam electrode can serve as a promising candidate for practical application of non-enzymatic glucose sensor.

Contributors

XIAO Qi provided the concept and reviewed the manuscript. ZHANG Yin-he analyzed the measured electrochemical data and wrote the original manuscript. HUANG Su-ping provided the concept and edited the draft of manuscript. All authors replied to reviewers' comments and revised the final revision.

Conflict of interest

ZHANG Yin-he, HUANG Su-ping and XIAO Qi declare that they have no conflict of interest.

References

[1] LI Hong-bo, ZHANG Ling, MAO Yi-wu, WEN Cheng-wei, ZHAO Peng. A simple electrochemical route to access amorphous Co-Ni hydroxide for non-enzymatic glucose sensing [J]. Nanoscale Research Letters, 2019, 14(1): 1−12. DOI: 10.1186/s11671-019-2966-2.

[2] WEI Ming, QIAO Yan-xia, ZHAO Hai-tao, LIANG Jie, LI Ting-shuai, LUO Yong-lan, LU Si-yu, SHI Xi-feng, LU Wen-bo, SUN Xu-ping. Electrochemical non-enzymatic glucose sensors: Recent progress and perspectives [J]. Chemical Communications (Cambridge, England), 2020, 56(93): 14553−14569. DOI: 10.1039/d0cc05650b.

[3] LIU Yue-jia, ZHAO Wen-qiang, LI Xian-liang, LIU Jia-qiang, HAN Yi-de, WU Jun-biao, ZHANG Xia, XU Yan. Hierarchical α-Fe_2O_3 microcubes supported on Ni foam as no n-enzymatic glucose sensor [J]. Applied Surface Science, 2020, 512: 145710. DOI: 10.1016/j.apsusc.2020.145710.

[4] DHARA K, MAHAPATRA D R. Electrochemical nonenzymatic sensing of glucose using advanced nanomaterials [J]. Microchimica Acta, 2017, 185(1): 1−32. DOI: 10.1007/s00604-017-2609-1.

[5] HWANG D W, LEE S, SEO M, CHUNG T D. Recent advances in electrochemical non-enzymatic glucose sensors− A review [J]. Analytica Chimica Acta, 2018, 1033: 1−34. DOI: 10.1016/j.aca.2018.05.051.

[6] HSIEH Y S, WANG P W, LI C Y, HSIEH S J, WANG C Y, CHOU D W, WANG N F, HOUNG M P. Fabrication of non-enzymatic Ni-Au alloy nanowire glucose sensor [J]. Sensors and Materials, 2020, 32(5): 1843−1850. DOI: 10.18494/SAM.2020.2479.

[7] YADAV H M, LEE J J. One-pot synthesis of copper nanoparticles on glass: Applications for non-enzymatic glucose detection and catalytic reduction of 4-nitrophenol [J]. Journal of Solid State Electrochemistry, 2019, 23(2): 503−512. DOI: 10.1007/s10008-018-4137-2.

[8] GUO Qi, ZENG Wen, LI Yan-qiong. Highly sensitive non-enzymatic glucose sensor based on porous $NiCo_2O_4$ nanowires grown on nickel foam [J]. Materials Letters, 2019, 256: 126603. DOI: 10.1016/j.matlet.2019.126603.

[9] ZHONG Shu-lin, ZHUANG Jun-yang YANG Da-peng, TANG Dian-ping. Eggshell membrane-templated synthesis of 3D hierarchical porous Au networks for electrochemical nonenzymatic glucose sensor [J]. Biosensors and Bioelectronics, 2017, 96: 26−32. DOI: 10.1016/j.bios.2017.04.038.

[10] KHUN K, IBUPOTO Z H, LIU X, BENI V, WILLANDER M. The ethylene glycol template assisted hydrothermal synthesis of Co_3O_4 nanowires; structural characterization and their application as glucose non-enzymatic sensor [J]. Materials Science and Engineering B—Advanced Functional Solid-State Materials, 2015, 194: 94−100. DOI: 10.1016/j.mseb.2015.01.001.

[11] LI Yao-yin, XIAO Qi, HUANG Su-ping. Highly active nickel-doped FeS_2 nanoparticles trigger non-enzymatic glucose detection [J]. Materials Chemistry and Physics, 2017, 193: 311−315. DOI: 10.1016/j.matchemphys.2017.02.051.

[12] XIAO Qi, WANG Xin-xin, HUANG Su-ping. Facile synthesis of $Ni(OH)_2$ nanowires on nickel foam via one step low-temperature hydrothermal route for non-enzymatic glucose sensor [J]. Materials Letters, 2017, 198: 19−22. DOI: 10.1016/j.matlet.2017.03.172.

[13] WANG Xin-xin, JIAN Hua-mei, XIAO Qi, HUANG Su-ping. In-situ fabrication of 3D flower-like NH_4NiPO_4 on Ni foam without nickel salts added for high sensitive nonenzymatic glucose detection [J]. Materials Research Bulletin, 2018, 100: 407−412. DOI: 10.1016/j.materresbull.2018.01.001.

[14] WANG Xin-xin, JIAN Hua-mei, XIAO Qi, HUANG Su-ping. Ammonium nickel phosphate on nickel foam with a Ni^{3+}-rich surface for ultrasensitive nonenzymatic glucose sensors [J]. Applied Surface Science, 2018, 459: 40−47. DOI: 10.1016/j.apsusc.2018.07.202.

[15] DONG Min, HU Hong-li, DING Shu-jiang, WANG Chang-cheng, LI Long. A facile synthesis of $CoMn_2O_4$ nanosheets on reduced graphene oxide for non-enzymatic glucose sensing [J]. Nanotechnology, 2021, 32(5): 055501. DOI: 10.1088/1361-6528/abc112.

[16] DAT P V, VIET N X. Facile synthesis of novel flower like Cu_2O nanowire on copper foil for a highly sensitive enzyme-free glucose sensor [J]. Materials Science & Engineering C—Materials for Biological Applications, 2019, 103: 109758. DOI: 10.1016/j.msec.2019.109758.

[17] ZHANG Chao, NI Hong-wei, CHEN Rong-sheng, ZHAN Wei-ting, ZHANG Bo-wei, LEI Rui, XIAO Tai-ping, ZHA Ya-xin. Enzyme-free glucose sensing based on Fe_3O_4 nanorod arrays [J]. Microchimica Acta, 2015, 182(9, 10): 1811−1818. DOI: 10.1007/s00604-015-1511-y.

[18] WANG Mei, SHI Ming-yu, MENG Er-chao, GONG Fei-long, LI Feng. Non-enzymatic glucose sensor based on three-dimensional hierarchical Co_3O_4 nanobooks [J]. Micro & Nano Letters, 2020, 15(3): 191−195. DOI: 10.1049/mnl.2019.0552.

[19] LI Zhan-hong, ZHAO Xue-ling, JIANG Xin-cheng, WU Yi-hua, CHEN Cheng, ZHU Zhi-gang, MARTY J L, CHEN Qing-song. An enhanced Nonenzymatic electrochemical glucose sensor based on copper-palladium Nanoparticles modified glassy carbon electrodes [J]. Electroanalysis, 2018, 30(8): 1803−1811. DOI: 10.1002/elan.201800017.

[20] MAO Wei-wei, HE Hai-ping, SUN Peng-cheng, YE Zhi-zhen, HUANG Jing-yun. Three-dimensional porous nickel frameworks anchored with cross-linked $Ni(OH)_2$ Nanosheets as a highly sensitive nonenzymatic glucose sensor [J]. ACS Applied Materials & Interfaces, 2018, 10(17): 15088−15095. DOI: 10.1021/acsami.8b03433.

[21] JIA Hui-xian, SHANG Ning-zhao, FENG Yue, YE Hui-min, ZHAO Jia-ning, WANG Huan, WANG Chun, ZHANG Yu-fan. Facile preparation of Ni nanoparticle embedded on mesoporous carbon nanorods for non-enzymatic glucose detection [J]. Journal of Colloid and Interface Science, 2021, 583: 310−320. DOI: 10.1016/j.jcis.2020.09.051.

[22] MA Min, ZHU Wen-xin, ZHAO Dong-yang, MA Yi-yue,

HU Na, SUO You-rui, WANG Jian-long. Surface engineering of nickel selenide nanosheets array on nickel foam: An integrated anode for glucose sensing [J]. Sensors and Actuators B — Chemical, 2019, 278: 110−116. DOI: 10.1016/j.snb.2018.09.075.

[23] DAI Hong-xiu, LIN Meng, WANG Nan, XU Fei, WANG Dong-lei, MA Hou-yi. Nickel-foam-supported Co_3O_4 nanosheets/PP_y nanowire heterostructure for non-enzymatic glucose sensing [J]. Chemelectrochem, 2017, 4(5): 1135−1140. DOI: 10.1002/celc.201600919.

[24] WANG Li, XIE Ying-zhen, WEI Chang-ting, LU Xing-ping, LI Xia, SONG Yong-hai. Hierarchical NiO superstructures/ foam Ni electrode derived from Ni metal-organic framework flakes on foam Ni for glucose sensing [J]. Electrochimica Acta, 2015, 174: 846−852. DOI: 10.1016/j.electacta.2015. 06.086.

[25] DIAZ-MORALES O, FERRUS-SUSPEDRA D, KOPER M T M. The importance of nickel oxyhydroxide deprotonation on its activity towards electrochemical water oxidation [J]. Chemical Science, 2016, 7(4): 2639−2645. DOI: 10.1039/ c5sc04486c.

[26] LI H B, YU M H, WANG F X, LIU P, LIANG Y, XIAO J, WANG C X, TONG Y X, YANG G W. Amorphous nickel hydroxide nanospheres with ultrahigh capacitance and energy density as electrochemical pseudocapacitor materials [J]. Nature Communications, 2013, 4: 1894. DOI: 10.1038/ncomms2932.

[27] LOUIE M W, BELL A T. An investigation of thin-film Ni−Fe oxide catalysts for the electrochemical evolution of oxygen [J]. Journal of the American Chemical Society, 2013, 135(33): 12329−12337. DOI: 10.1021/ja405351s.

[28] SINGER N, PILLAI R G, JOHNSON A I D, HARRIS K D, JEMERE A B. Nanostructured nickel oxide electrodes for non-enzymatic electrochemical glucose sensing [J]. Microchimica Acta, 2020, 187(4): 1−10. DOI: 10.1007/ s00604-020-4171-5.

[29] HE Ge-ge, TIAN Liang-liang, CAI Yan-hua, WU Shen-ping, SU Yong-yao, YAN Heng-qing, PU Wan-rong, ZHANG Jin-kun, LI Lu. Sensitive Nonenzymatic electrochemical glucose detection based on hollow porous NiO [J]. Nanoscale Research Letters, 2018, 13(1): 1−10. DOI: 10.1186/ s11671-017-2406-0.

[30] ZHANG Yi, ZHAO Dong-yang, ZHU Wen-xin, ZHANG Wen-tao, YUE Zhi-hao, WANG Jing, WANG Rong, ZHANG Dao-hong, WANG Jian-long, ZHANG Guo-yun. Engineering multi-stage nickel oxide rod-on-sheet nanoarrays on Ni foam: A superior catalytic electrode for ultrahigh-performance electrochemical sensing of glucos [J]. Sensors and Actuators B—Chemical, 2018, 255: 416−423. DOI: 10.1016/j.snb.2017.08.078.

[31] JAFARIAN M, FOROUZANDEH F, DANAEE I, GOBAL F, MAHJANI M G. Electrocatalytic oxidation of glucose on Ni and NiCu alloy modified glassy carbon electrode [J]. Journal of Solid State Electrochemistry, 2009, 13(8): 1171−1179. DOI: 10.1007/s10008-008-0632-1.

[32] LIU Hong-yu, LU Xing-ping, XIAO De-jian, ZHOU Min-xian, XU Du-jian, SUN Lan-lan, SONG Yong-hai. Hierarchical Cu–Co–Ni nanostructures electrodeposited on carbon nanofiber modified glassy carbon electrode: application to glucose detection [J]. Analytical Methods, 2013, 5(22): 6360−6367. DOI: 10.1039/c3ay41170b.

[33] PADMANATHAN N, SHAO H, RAZEEB K M. Multifunctional nickel phosphate nano/microflakes 3D electrode for electrochemical energy storage, Nonenzymatic glucose, and sweat pH sensors [J]. ACS Applied Materials & Interfaces, 2018, 10(10): 8599−8610. DOI: 10.1021/ acsami.7b17187.

(Edited by ZHENG Yu-tong)

中文导读

无酸一步法合成高度分散铁元素修饰的泡沫镍无酶葡萄糖传感器

摘要：本文提出了一种简单而有效的方法将泡沫镍电极改性并用于无酶葡萄糖传感器。在室温、无酸的条件下，将泡沫镍浸入硝酸铁溶液中制备高分散的铁元素修饰的电极，并通过 X 射线粉末衍射(XRD)，扫描电子显微镜(SEM)，EDAX 光谱(EDAX)和拉曼光谱进行表征。EDAX 光谱表明，铁元素高度分散在泡沫镍的整个表面上；拉曼光谱表明，Ni—O 和 Fe—O 键均在制备好的电极表面上形成。此外，铁元素修饰的泡沫镍电极不仅具有 1~18 mmol/L 的超宽线性浓度范围和 1.0388 mA·mmol/(L·cm^2)的灵敏度，还具有很强的稳定性和选择性，可以用作非酶葡萄糖传感器。

关键词：一步合成法；无酸处理；高度分散的铁元素；泡沫镍；无酶葡萄糖传感器